Arctic Shelf and Large Rivers Seamless Nesting in Global HYCOM

Eric Chassignet
Center for Ocean-Atmosphere Prediction Studies (COAPS)
Florida State University, PO Box 3062840
Tallahassee, FL 32306-2840
phone: (850) 645-7288 fax: (850) 644-4841 email: echassignet@fsu.edu

Award Number: N00014-15-1-2594

LONG-TERM GOALS

Fresh water inputs such as rivers and ice melt are poorly represented in global HYCOM since many of the processes associated with river plume dynamics and ice melt are unresolved. The main scientific and technical objective of the proposed work is to implement river mass flux and temperature flux boundary conditions, as well as two-way nesting to improve the representation of large river plumes and Arctic Ocean ice melt water runoff (land ice and glacier) in global HYCOM and to improve the predictability in coastal regions, the Arctic Ocean, and the Atlantic Ocean. To assess the fidelity of the inner nests and boundary conditions, we will compare our simulations to all available observations. Emphasis will be placed on the fresh water plume dynamics and offshore circulation dynamics, as well as how the rivers impact the seasonal ice melt. We anticipate that the more accurate treatment of the river inflow and embedded two-way nested higher resolution local models will translate into improved river plume dynamics.

OBJECTIVES

The overall goal of this work is to investigate the fate and pathways of fresh water in the pan-Arctic system in order to assess the role of fresh water in the current changes of the Arctic ocean–sea ice system. The technical objective of the proposed work is to implement two-way nesting in HYCOM that will improve the representation of the large river plumes and ice melt water runoff (land ice and glacier) in coastal areas of the global and Arctic Cap HYCOM in order to advance the predictability in coastal regions, the Arctic Ocean, and the sub-Arctic seas.

The specific objectives are to:

- Evaluate the performance of the GOFS and Arctic Cap using available hydrographic and sea ice observations in terms of ocean basin-scale circulation, distribution of major water masses with particular focus on the Beaufort Gyre, and characteristics of sea ice on the shelf and interior basin.
- Implement river mass flux and temperature flux boundary conditions to HYCOM.
- Develop and evaluate a two-way HYCOM-HYCOM nesting.
- Implement coupled CICE in nested HYCOM system.
- Parameterize land-fast ice in HYCOM.
- Apply two-way nested modeling systems to:

  - investigate and improve the fate and pathways of river and meltwater runoff on the Arctic shelves, coastal region, Arctic Ocean, and sub-Arctic seas;
  - quantify the impact of fresh water on thermohaline processes on the Arctic shelves such as convection and water mass formation, heat exchange between deep and upper ocean layers, sea ice formation and melting;
  - assess the impact of fresh water input on the Arctic Ocean mixed layer (depth, thermohaline characteristics, water column stability).
  - evaluate sea ice formation and melting processes on the shelf under different fresh water content conditions.
  - analyze the fresh water plume dynamics in the two-way nested models and compare it to the current GOFS HYCOM; and
  - explore parameterizations of the fresh water dynamics and mixing implicitly resolved by the high-resolution shelf nests for the coarser global model to improve simulation and predictability of the shelf processes.
- Evaluate the benefit of using a nested super-high resolution (<500 m) model of the Arctic shelf seas with the unstructured-grid Finite-Volume Community Ocean Model (FVCOM) instead of a HYCOM-HYCOM nest.
- Incorporate HYCOM (replacing NCOM) in the COAMPS Arctic System.

The above objectives are to be realized in partnership with the Naval Reserach Laboratory (see separate report by P. Hogan)

APPROACH

Simulation of the hydrodynamic processes on the Arctic shelves is challenging due to a number of factors. Among these are: coastal line with a complex geometry, presence of land-fast ice, seasonal ice cover, formation of polynyas and formation of water masses. Estimates of the baroclinic deformation (Rossby) radii have small (<1 km) values over most of the Arctic shelves. In order to adequately describe boundary currents, river plumes, and the eddy field, a model horizontal resolution should be at least two grid points per Rossby radius of deformation. The proposed approach will be to use two-way nesting to quantify the impact of a better representation of fresh water pathways on the Arctic shelves and fresh water flux to the Arctic interior. First, a high resolution (O(1 km)) HYCOM-to-HYCOM nest will be implemented, not only to provide better resolution of the shelves but also to improve river mass and temperature fluxes. The configuration will allow for the quantification of the impact of a better representation of fresh water pathways on the Arctic shelves and fresh water flux to the Arctic interior. Then, the benefit of using a nested super-high resolution (< 1 km with less than 500 m near the coast) model of the Arctic shelf seas with the unstructured-grid Finite-Volume Community Ocean Model (FVCOM) instead of a HYCOM-HYCOM nest will be evaluated. Both nested shelf models will have improved representation of the river runoff including mass flux and heat flux associated with river water temperature. The nested modeling systems will be evaluated against in situ and satellites observations (ocean color, sea ice extent). The developed two-way nested modeling system will be employed to: (1) determine transport pathways and fate of fresh water on the shelves, (2) characterize ocean-shelf fresh water flux, and (3) evaluate the influence, over the Arctic shelves, of continental runoff on thermohaline processes and sea ice formation. The results from the nested models will be compared to the outputs from the current Arctic Cap and global HYCOM in order to assess the benefit of high-resolution nesting of the shelf regions.

WORK COMPLETED

Task 1: Validation and improvements of existing Arctic HYCOM simulations

During the past year, we pursued the validation of the Global HYCOM+NCODA Reanalysis and Analysis, focusing on the accuracy of the Mixed Layer Depth (MLD) representation in the Arctic Ocean and Subpolar North Atlantic. The accuracy of the upper-ocean characteristics depends on the turbulent mixing schemes implemented in a model, surface buoyancy flux, momentum flux, and wave stresses (usually parameterized in the turbulence schemes) and the MLD and its characteristics (T, S, and dynamics) is a usual variable that is commonly used to validate the accuracy of the simulated upper-ocean characteristics.

The model climatology of MLDs in the Arctic Ocean and Subpolar North Atlantic is estimated from the Global HYCOM+NCODA Reanalysis and Analysis (GLBb0.08) for 1993-2015 by evaluating different definitions of the MLDs in order to determine the most robust technique applicable for the high-latitudinal seas. Specifically, the methods suggested by Kara et al. (2000) and Boyer Montegut et al. (2004) as well as methods based on a threshold criteria (e.g., Monterey and Levitus, 1997) are not reliable for polar and subpolar oceans. The problem is related to the very small temperature range in the Arctic region and the pre-defined threshold value for T that is used to calculate the expected density at the base of the mixed layer (Kara et al., 2000). In Kara et al. (2000), the MLD algorithm is based on ΔT and the threshold reference temperature T_{REF}. In the Arctic, this can lead to erroneously deep mixed layer all the way to the bottom. An alternative approach was developed that selects threshold value of ΔT (that is used to calculate the mixed layer density to find the MLD) individually for each profile considering statistics of T values in the water column. Preliminary results are shown for the select regions shown in Figure 1. The two methods agree well in the interior Arctic Ocean due to strong stratification and a well pronounced pycnocline and differ mostly subpolar North Atlantic regions, where the MLD has large spatial and temporal variability (Figure 2). The MLDs are currently being compared to in situ observations and Argo profiles (collaboration with St. Petersburg State University).

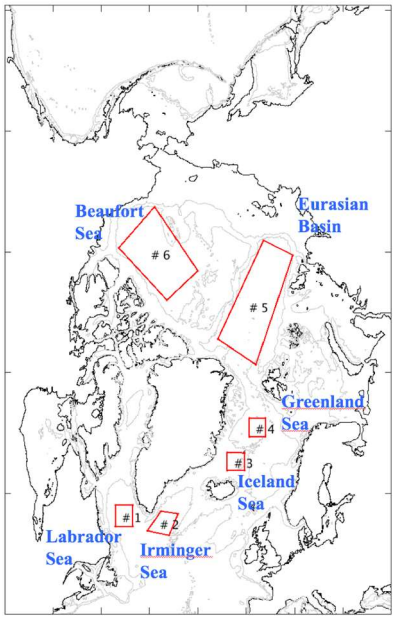

Figure 1. Regions where the MLD from HYCOM reanalysis is evaluted and compared to observations.

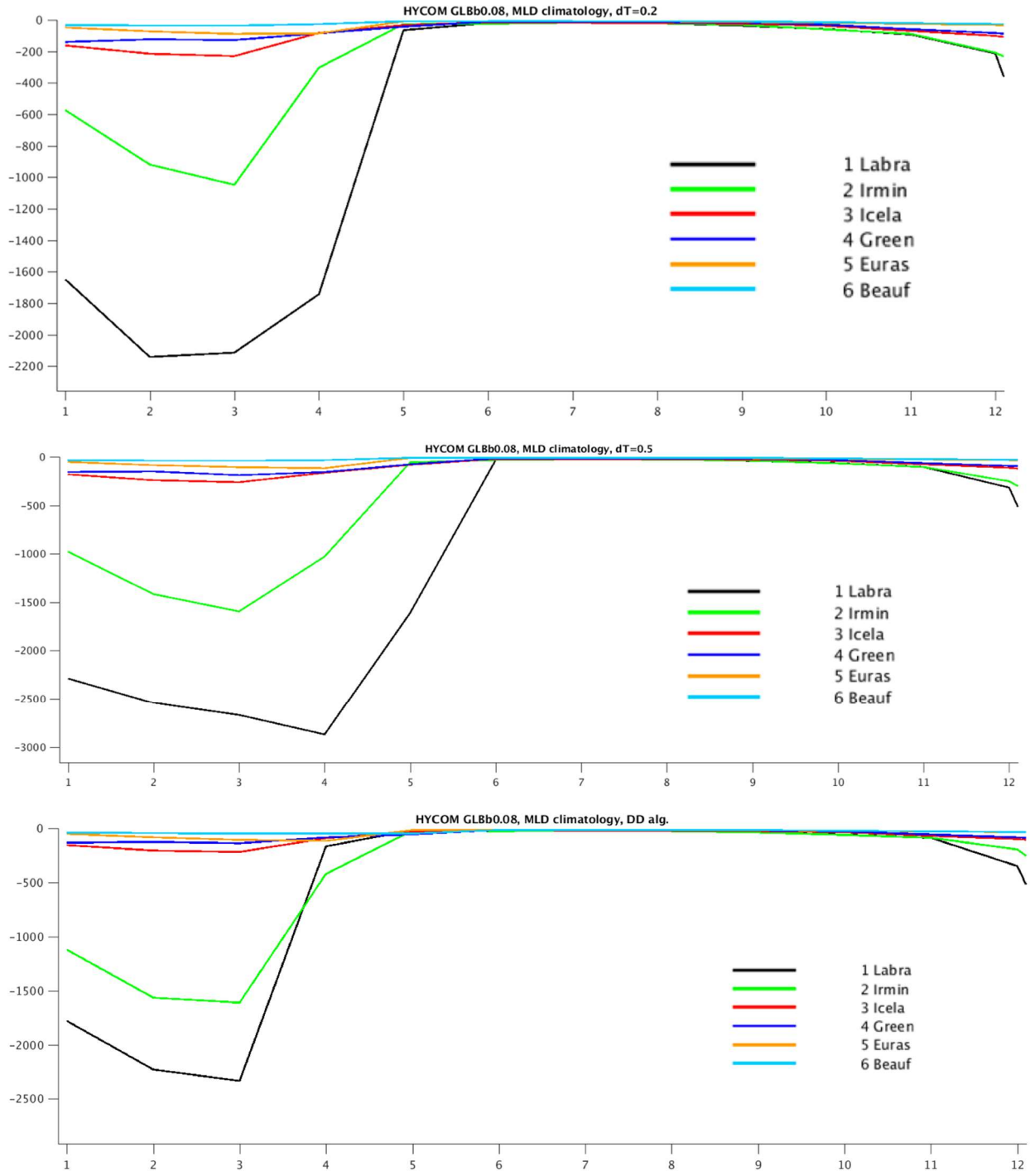

Figure 2. MLD climatology from HYCOM reanalysis for 6 regions (red boxes in Figure 1) estimated using Kara et al. [2000] and the alternate method. For Kara methodology, dT = 0.2C (top) and 0.5C (middle).

Task 2: Freshwater pathways in the Arctic and sub-Arctic seas

We investigate the pathways of fresh water in the Arctic Ocean and North Atlantic in a series of experiments with increasing complexity, 0.08º and 0.04º, wiyth and without improved water runnoff over the Arctic.

a) Numerical Experiment 11.0 with 0.08 AO HYCOM (Control Run)

We use the 0.08º coupled HYCOM-CICE configured for the Arctic Ocean domain with improved bathymetry and vertical grid. The model is nested into the Global HYCOM Reanalysis/Analysis and is integrated during 1993-2015. In order to track propagation of fresh water, 5 passive tracers are constantly released during the simulation at the major sources of fresh water in the Arctic Ocean and Greenland (Figure 3). The amount of tracer prescribed at every location is proportional to the fresh water flux in the model, including Greenland coast (~400 fresh water sources along the course). This allows one to quantify the contribution of different fresh water sources to the Artic Ocean fresh water budget as well as fresh water fluxes between different regions in the Arctic Ocean and the North Atlantic. Passive tracers allows accurate tracking of fresh water from its source to the interior regions of the Arctic Ocean and to the North Atlantic. It should be mentioned that this effort contributes to the international modeling experiment investigating Greenland and Arctic fresh water pathways withing FAMOS, led by D. Dukhovskoy (FSU/COAPS). In the control simulation, river runoff in the Arctic and North Atlantic in the model is prescribed similar to the existing 0.08-degree Global HYCOM reanalysis/analysis. This is river climatology in the Arctic Ocean and no Greenland runoff. The preparation of the nest fields, restart fields, the set up and configuration of the model were described in the annual report of 2016. The model experiment has been successfully completed (Figure 4) and the output will be analyzed in the coming year.

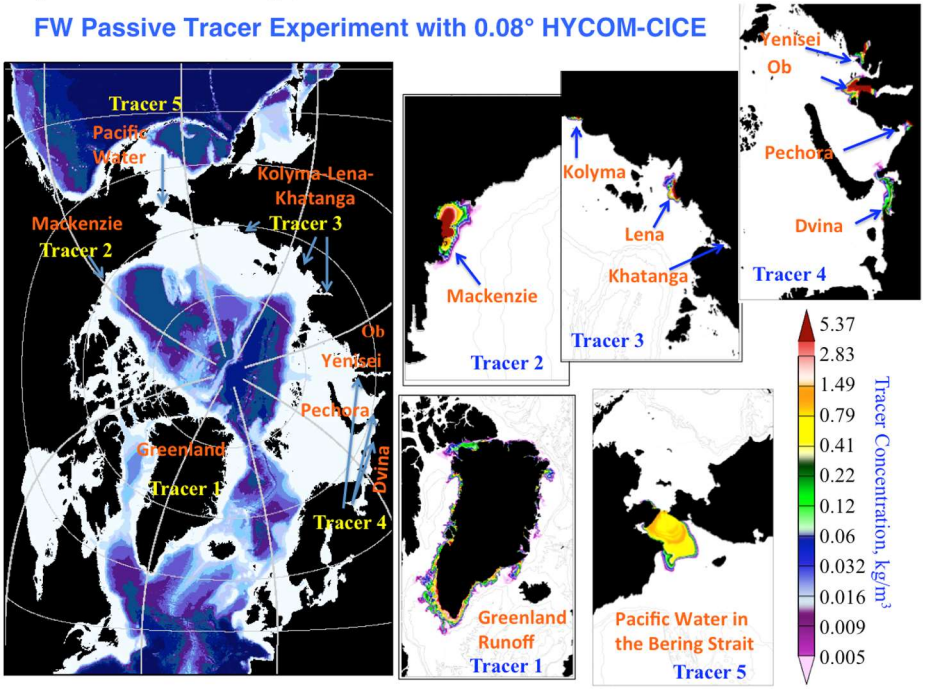

Figure 3. Release locations of fresh water passive tracers in the 0.08 AO HYCOM-CICE simulation. Colors indicate fresh water tracer concentration (kg/m3).

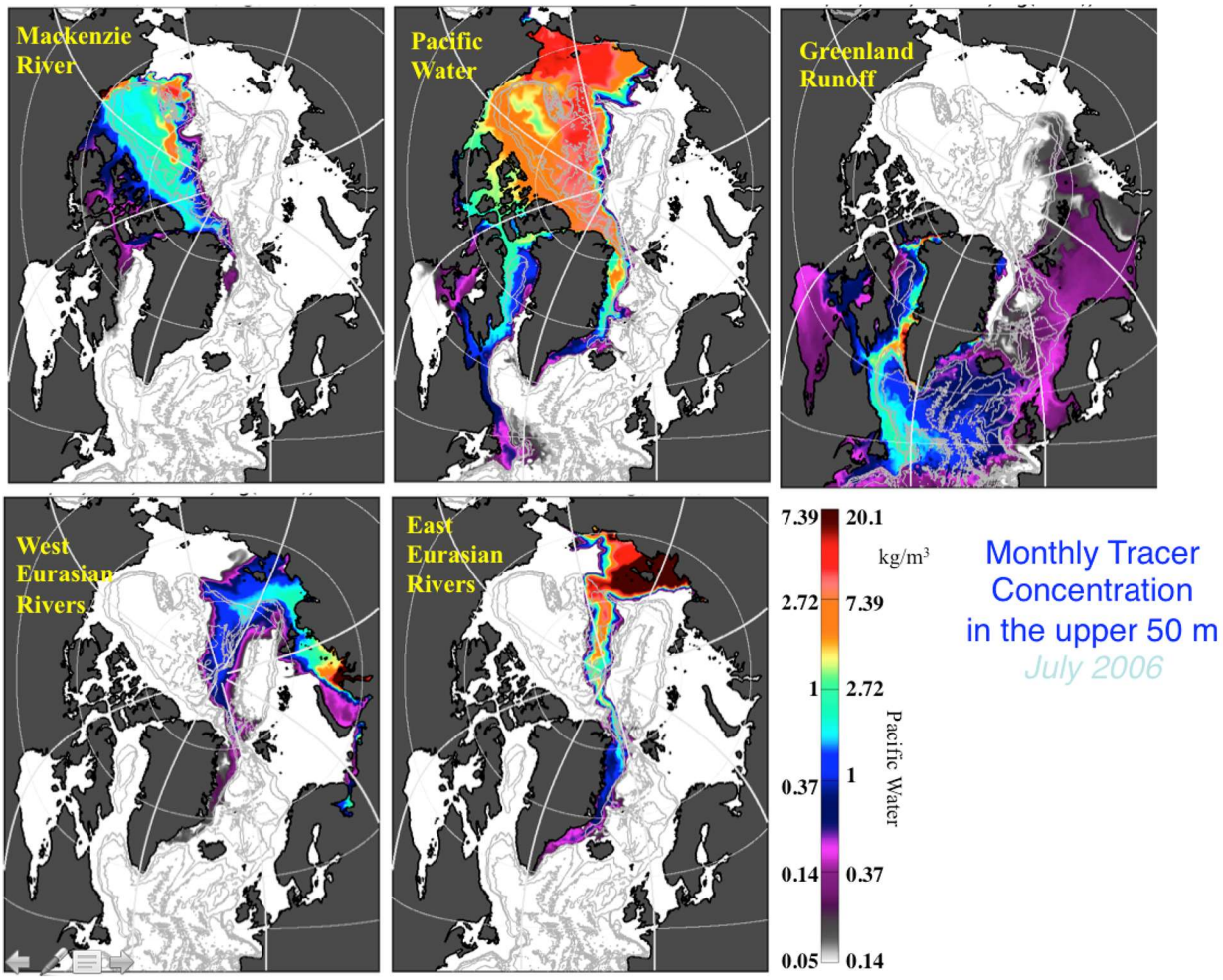

Figure 4. Preliminary results from the 0.08 AO HYCOM-CICE tracer experiment. The figure shows concentration of the individual tracers after 13.5 years of the model run. The colors are tracer concentration (logarithmic scale), kg/m3.

b) Numerical Experiment 0.08 AO HYCOM (epxt 11.2) with and improved river runoff

The main objective of this experiment is to analyze the impact of improved river runoff and Greenland fresh water flux on numerical solution (dynamics and thermohaline characteristics) in the coastal and shelf regions. The model setup is identical to the control run (including the allocation and prescribed flux of the passive tracers). The main difference is improved representation of the river runoff in the Arctic Ocean and along the Greenland coast. River monthly mean discharge rates have been created for the Arctic Ocean and the North Atlantic on the basis of NCAR/UCAR CGD data set. The total number of rivers (without Greenland fresh water sources) is 72 (vs 30 in the control run). An algorithm has been created for automatic quality control of the data, gap filling, and distribution in the model grid. All river locations have been validated and corrected as necessary (Figure 5). Greenland freshwater sources are incorporated into AO-HYCOM using monthly inter-annual gridded data (Bamber et al., 2012) (see Figure 6). The model experiment is currently being integrated.

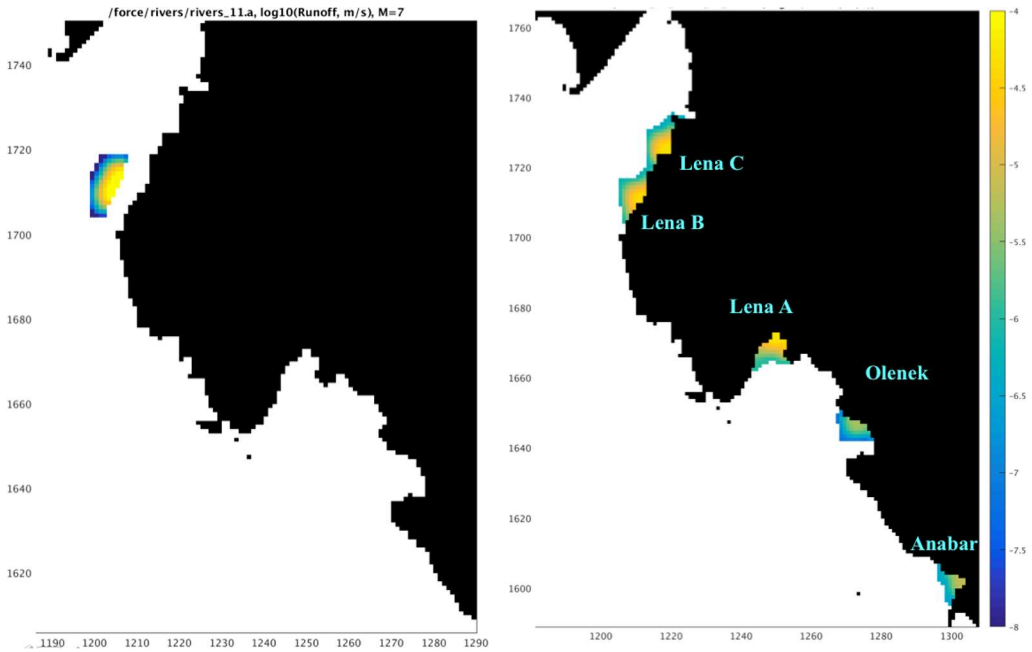

Figure 5. River sources in the Laptev Sea in the HYCOM experiment 11.0 (control run, left) and 11.2 (right).

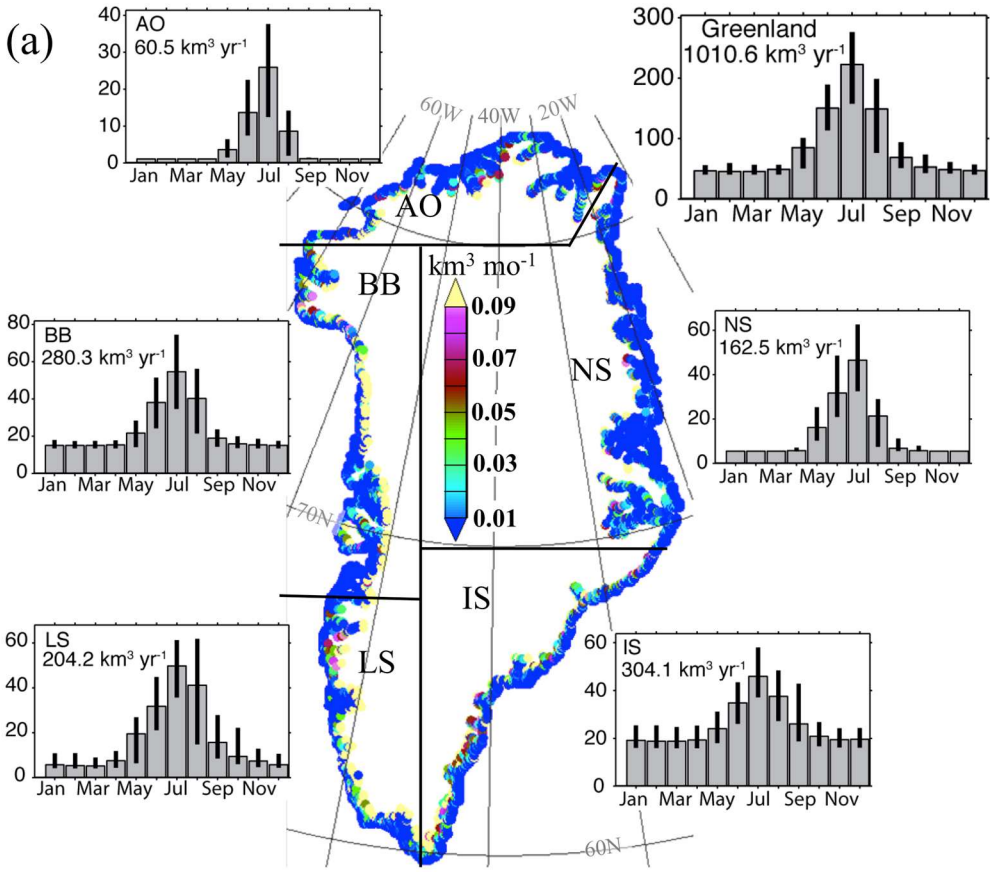

Figure 6. Locations of the individual Greenland fresh water sources (Dukhovskoy et al., 2016).

c) Numerical Experiment 0.04 AO HYCOM (epxt 01.0, 01.1)

The main objective of this experiment is to investigate the role of the small mesoscale dynamics (in the order of baroclinic Radius of deformation that is in the order 2 km on the Arctic and Greenland shelves) on fresh water and heat fluxes in the Arctic Ocean and Subpolar North Atlantic. We therefore configured a high-resolution (0.04º, ~ 2km in the Arctic Ocean) configuration of the AO HYCOM-CICE. The steps we undertook are

1) Model grid and bathymetry for 0.04-degree configuration have been prepared. The erroneously closed Fary and Heccla strait has been opened (Figure 7).
2) Model restart fields are interpolated into 0.04-degree grid from 0.08 AO HYCOM-CICE experiment 11.0 (January 1, 2005). Tracer fields are interpolated into the 0.04-degree grid and saved into the restart data file.
3) CICE restart fields are prepared from 0.08 AO HYCOM-CICE experiment 11.0 (January 1, 2005).
4) An algorithm for preparing lateral OB forcing ("nest") fields from Global HYCOM Reanalysis/Analysis has been prepared.
5) Test simulation without surface and lateral OB forcing has been performed.
6) Test simulation with all forcing fields turned "on" has been performed for 10 months of 2005 (Figure 8). The high-resolution simulation reveals better representation of baroclinic instabilities along the oceanic fronts, propagation of the fresh water plumes, and smaller scale eddies in the study region.

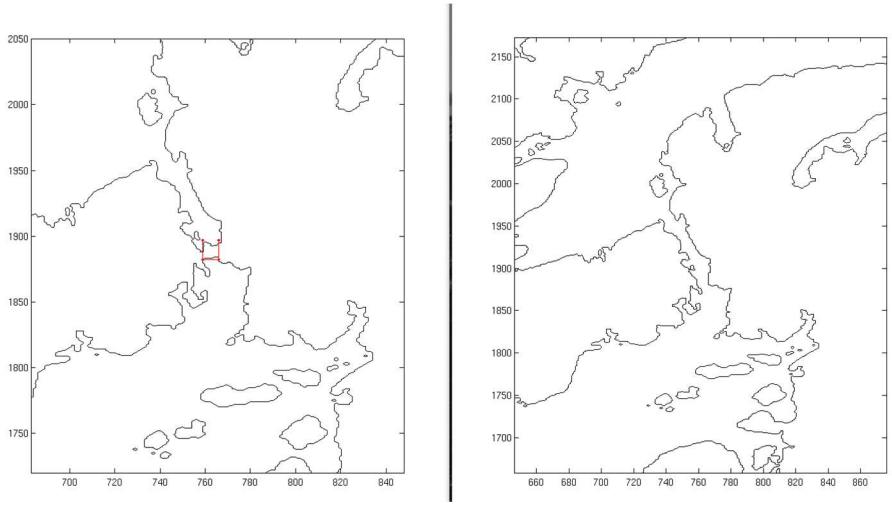

Figure 7. Closed Fary and Heccla strait in Topography T17 (left) has been opened in corrected version of T17 (right).

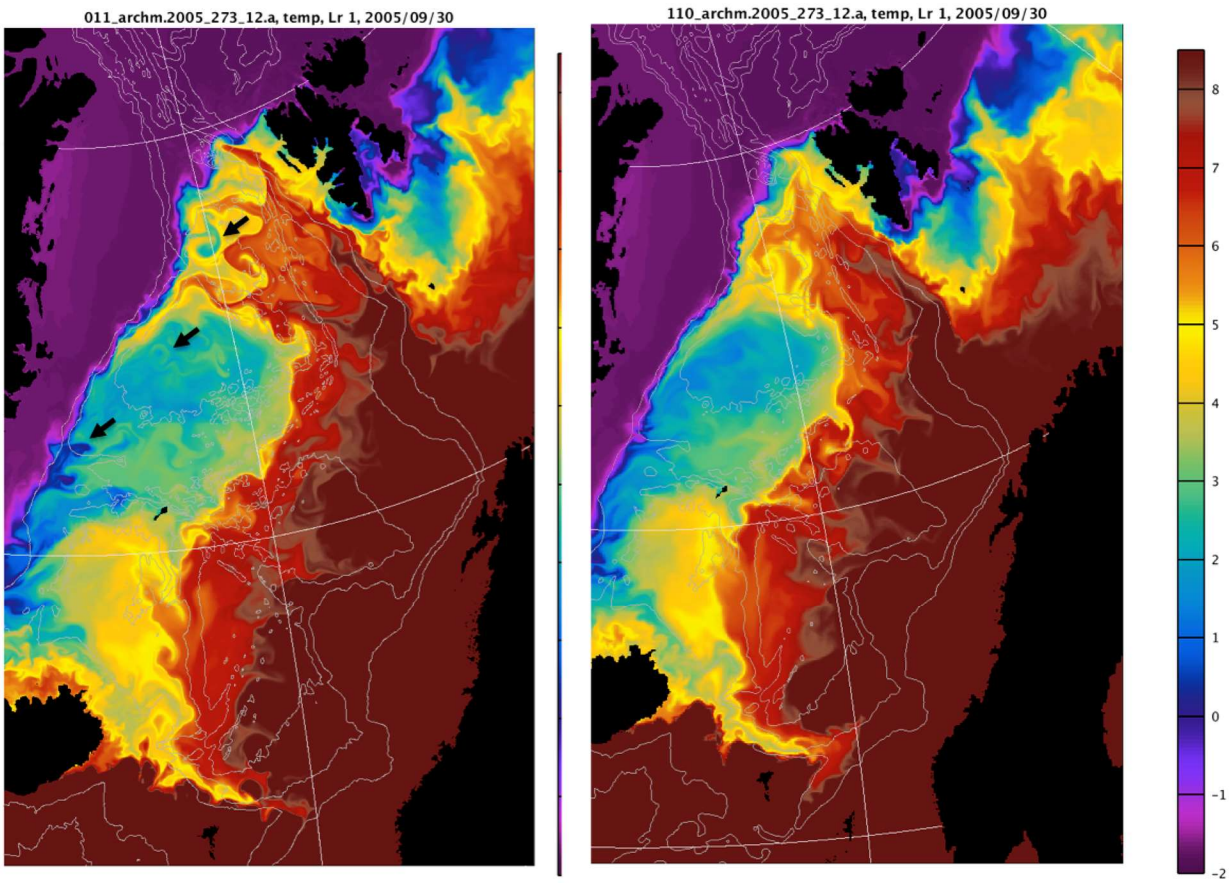

Figure 8. Simulated near-surface T fields in the 0.04 AO HYCOM-CICE (left) and 0.08 AO HYCOM-CICE (right).

Task 3: Implement river mass flux and temperature flux boundary conditions to HYCOM.

Testing of HYCOM River Parameterizations in Idealized Simulations

A suite of idealized HYCOM simulations have been run based on configurations found in the literature to test several aspects of river plumes simulated with different parameterizations of rivers that are presently implemented in HYCOM. The idealized model configuration is designed to replicate that used by Hetland (2005) to study near-field plume dynamics with ROMS, which is also similar to several other previous studies. Modifications of this idealized estuary-shelf configuration are also used to understand the impact of different river parameterizations in more typical implementations of rivers in large-scale HYCOM simulations.

The model configuration used here has a 1-km resolution grid over a 300km long, 75km wide shelf on an *f*-plane at 45°N (Figure 9). The bottom slope is 1/1500, with a maximum depth of 70m. The temperature is initially 20°C in the upper 10m, decreasing to 5°C at depth with a 20m decay scale. A single river source of 1000 m^3/s enters the domain either through a 25km-long 3km-wide estuary normal to the coast. In a modified idealized simulation, the river inputs to the shelf directly adjacent to the straight coastline with no estuary, a more typical implementation of river sources in large-scale

HYCOM simulations. This configuration uses closed lateral boundaries, but analysis of the simulation is confined to the time before the river plume begins interacting with the boundaries.

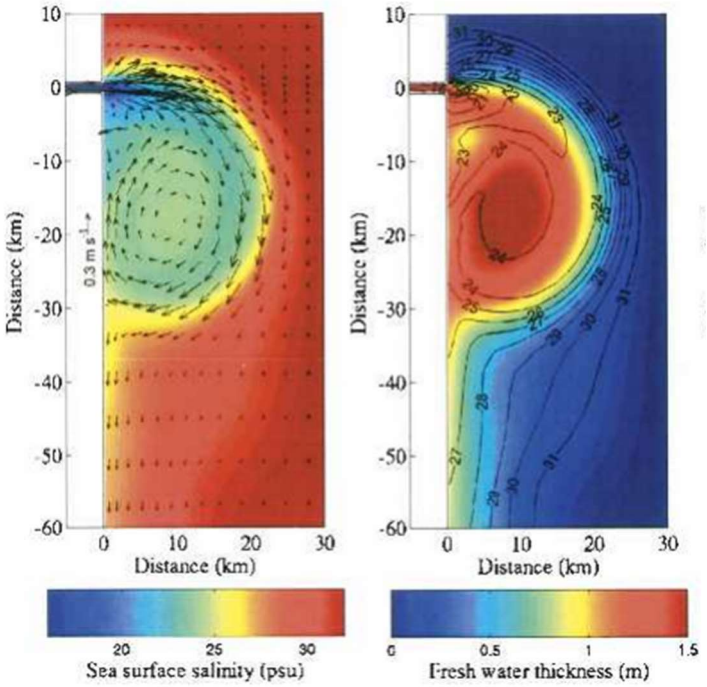

Figure 9. Left: Surface salinity field simulated with a 1000 m^3/s river source in a idealized shelf configuration of the ROMS model from Hetland (2005). Right: Freshwater thickness from the same simulation

Three different parameterizations are being tested in this study. The first parameterizes riverine input as a surface salinity flux prescribed as a bogus precipitation over a region about the river source. The second provides an mass flux associated with the bogus precipitation that can through modification of the pressure. This effectively can provide a mass source distributed with some depth profile as opposed to being constrained to the topmost grid cell. The last is a recently implemented option in which river sources are simulated as a volume flux with prescribed temperature and salinity at port locations.

The three-dimensional plume structure is analyzed for the different model configurations using bogus surface precipitation parameterization for rivers with and without associated mass flux. Simulations parameterizing riverine inflow using port forcing (lateral volume flux with prescribed temperature and salinity) are yielding numerically unstable solutions at this time and further testing of the model code is ongoing. Each of the simulations produces a large-scale (far-field) salinity pattern characteristically similar to that of Hetland (2005) – that is, a roughly 20km bulge turning anticyclonically toward the coast and then a coastal jet flowing with the coast to the right. The surface salinity fields for the experiments having an idealized estuary appear very similar (Figure 10). The models with rivers source along the coast (no estuary) have weaker gradients and generally higher salinities within the plume indicative of the plumes being too diffuse (overly mixed) compared to the models with river sources inside a simple channel-like estuary. The model with estuary that uses the mass flux parameterization has a lower salinity in the core of the jet compared to the model that uses the bogus precipitation with no mass flux.

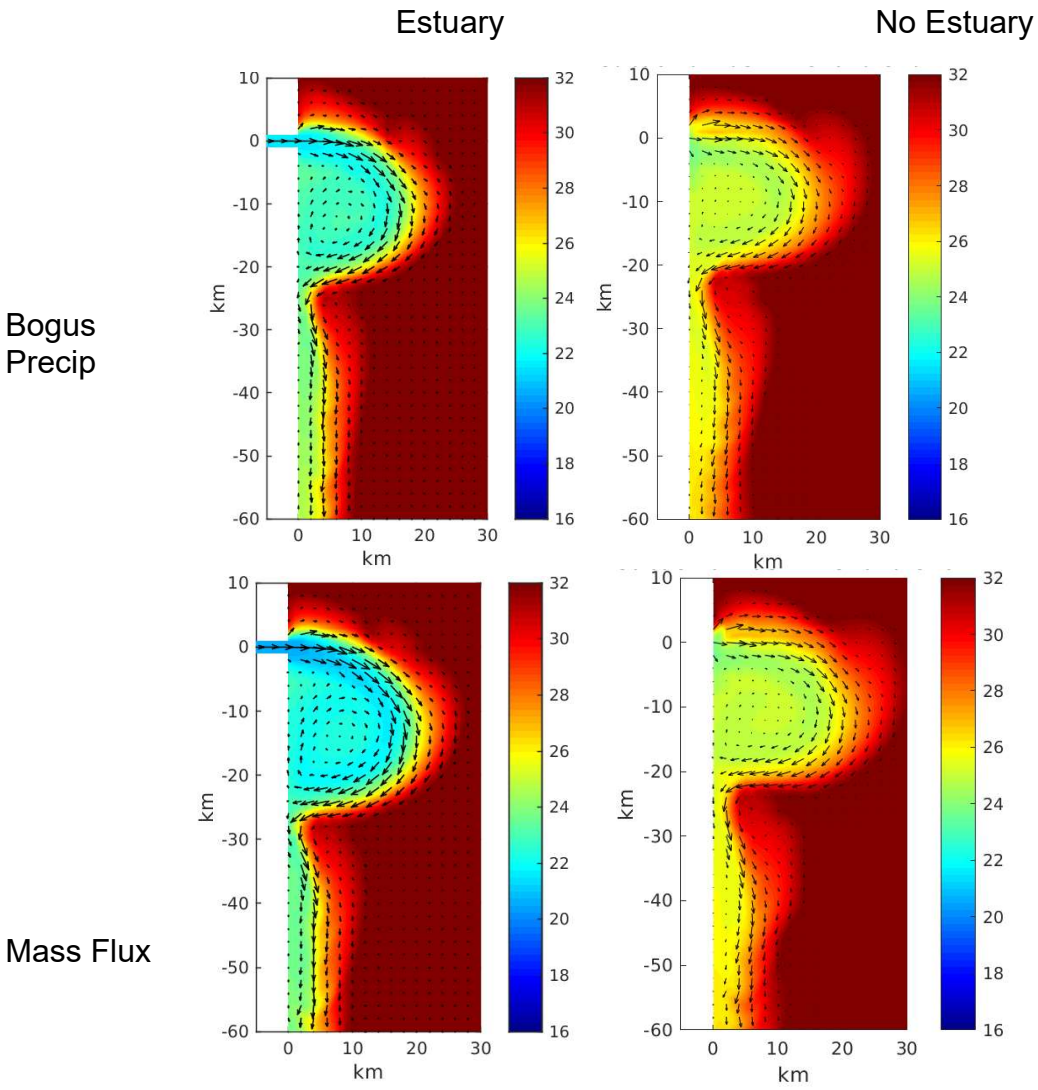

Figure 10. Surface salinity fields after 16 days of integration from simulations having an idealized estuary (left) or river input adjacent to the coast with no estuary (right). Rivers are parameterized as bogus surface precipitation (top) with associated mass flux (bottom).

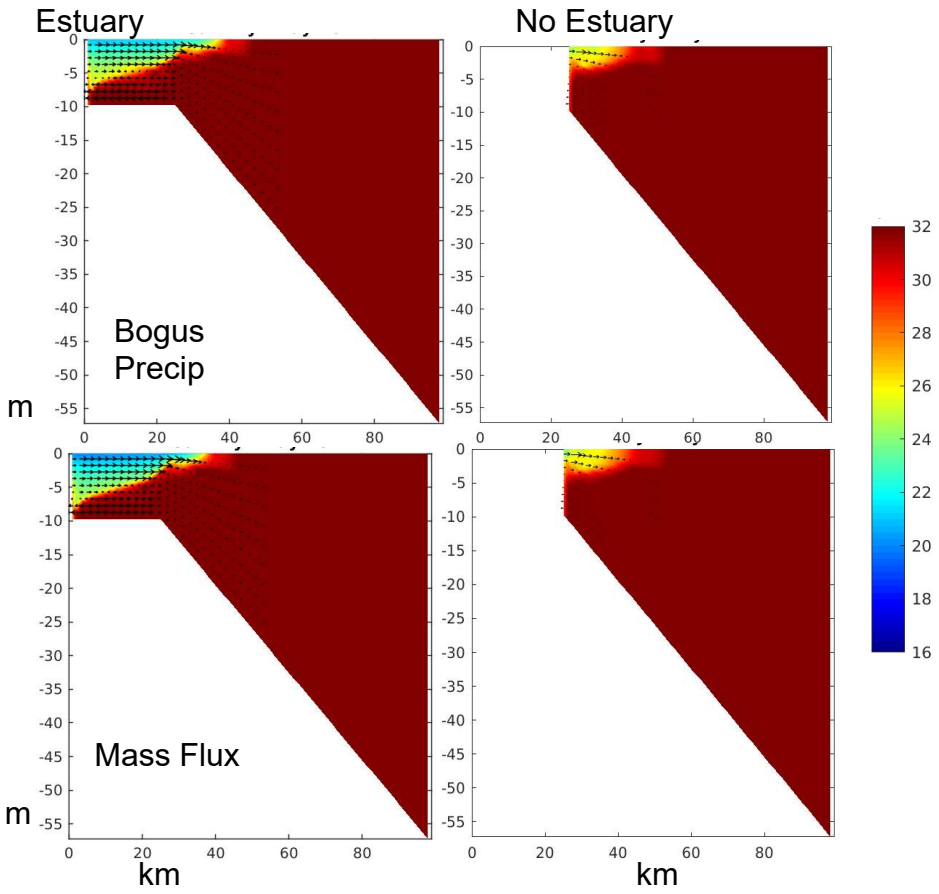

Figure 11. Vertical sections of salinity after 16 days of integration from simulations having an idealized estuary (left) or river input adjacent to the coast with no estuary (right). Rivers are parameterized as bogus surface precipitation (top) with associated mass flux (bottom).

The vertical structure of the salinity field along a section normal to the coast passing through the location of the river source again shows similarities in both models with estuaries (Figure 11). These simulate a baroclinic estuarine flow structure (inflow at depth, outflow at surface), resulting in a wedge-type estuary. The simulations with rivers input directly along the coastline (no estuary) both yield markedly weaker stratification. The flow normal to the coast under the plume is also much weaker in these simulations than in the simulations with estuaries. The plumes are thicker over the shelf in the simulations with no estuary. This is manifest as larger freshwater thickness (computed as the vertical integral of the salinity anomaly from a reference of 32) over the shelf adjacent to the coast in the simulations with no estuary compared to those with riverine input to the shelf occurring via an estuary (Figure 12). When the river is input to an estuary, the maximum freshwater thickness within the bulge is separated from the coast, consistent with the pattern shown by Hetland et al. (2005) (Figure 8). Freshwater thickness within the plume bulge is also greater for the experiments parameterizing the mass flux associated with the river input than in those experiments that prescribe rivers solely as a surface salinity flux.

The relatively diffuse plume simulated in the experiments with river input directly at the coast is associated with along-plume jets that are generally weaker and broader than the model experiments with rivers input through estuaries (Figure 13). The outflow from the estuary is stronger in the model

with mass flux parameterization than the model without. Despite the fact that both simulations with estuaries produce similar-looking outflow of low salinity water, the actual volume flux in the experiment with no compensating mass flux to the surface salinity flux is zero. The simulation with the mass flux parameterization provides nearly the prescribed riverine volume flux at the mouth of the estuary (932 m^3/s versus a prescribed value of 1000 m^3/s) (Figure 14). Upcoming work will further analyze the salinity flux simulated with the different riverine parameterizations. Once the implementation of rivers as port forcing is corrected, thermal fluxes associated with the rivers will also be analyzed.

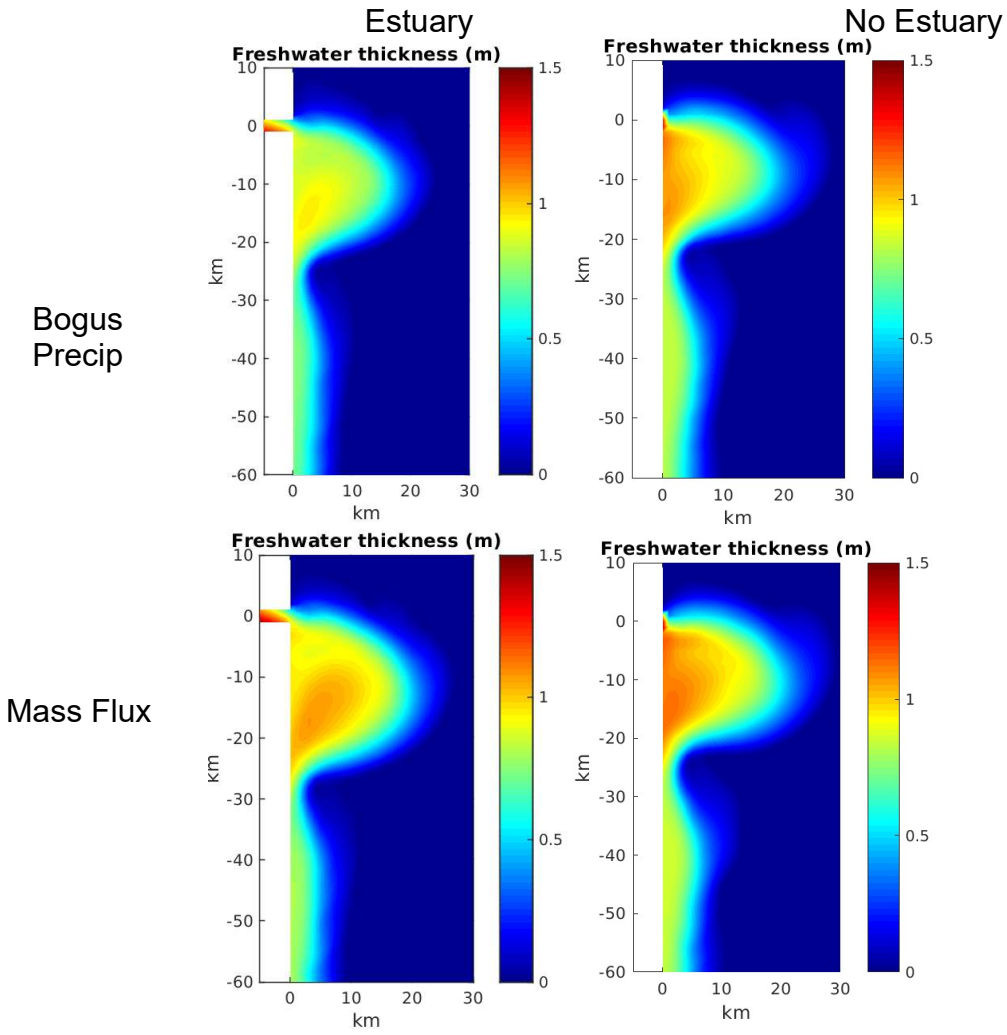

Figure 12. Freshwater thickness computed as the vertical integral of the salinity anomaly after 16 days of integration from simulations having an idealized estuary (left) or river input adjacent to the coast with no estuary (right). Rivers are parameterized as bogus surface precipitation (top) with associated mass flux (bottom).

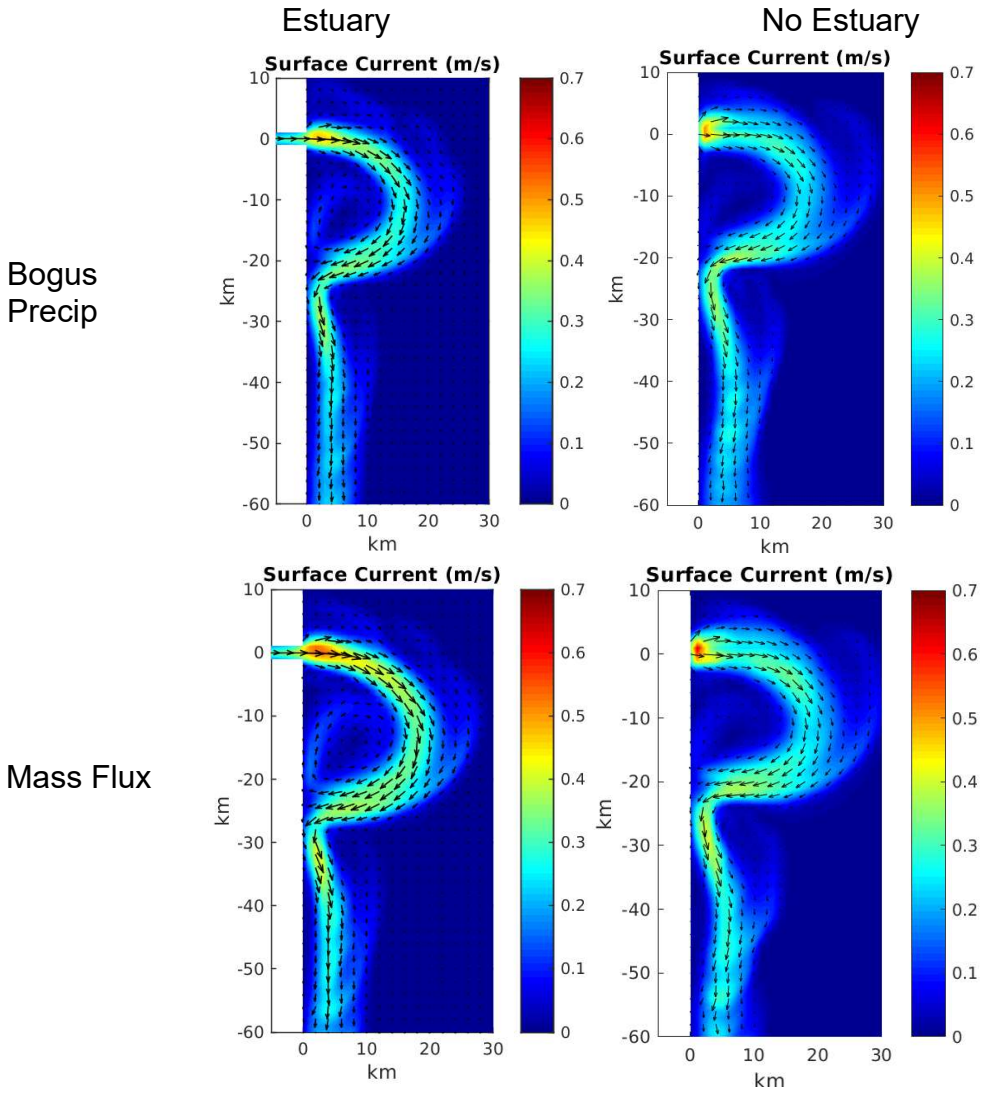

Figure 13. Surface velocity fields after 16 days of integration from simulations having an idealized estuary (left) or river input adjacent to the coast with no estuary (right). Rivers are parameterized as bogus surface precipitation (top) with associated mass flux (bottom).

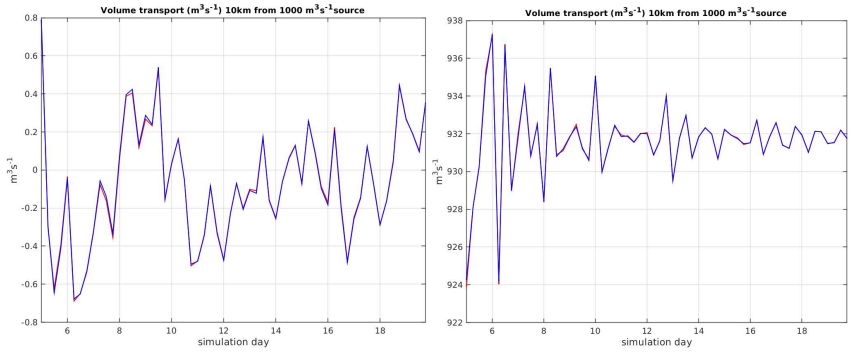

Figure 14. Time series of volume transport at the mouth of the estuary computed from the simulation with rivers parameterized as surface salinity flux only (left) and with an associated mass flux (right).

RESULTS

- Validation of 1/12° HYCOM global reanalysis (GLBb0.08) from 1993 to 2012.
- Configuration of a 0.08-degree coupled HYCOM-CICE for the Arctic Ocean to study freshwater pathways

RELATED PROJECTS

This project builds on the core model development activities taking place at the Naval Research Laboratory (see annual report by P. Hogan).

REFERENCES

Boyer Montegut, C., G. Madec, A.S. Fischer, A. Lazar, and D. Iudicone, 2004. Mixed layer depth over the global ocean: An examination of profile data and a profile-based climatology. J. Geophys. Res., 109, C12003, doi:10.1029/2004JC002378.

Hetland, R.D., 2005. Relating river plume structure to vertical mixing. J. Phys. Oceanogr., 35 (9), 1667-1688.

Kara, A. B., P. A. Rochford, and H. E. Hurlburt, 2000. An optimal definition for ocean mixed layer depth, J. Geophys. Res., 105, 16,803 – 16,821.

Monterey, G. and Levitus, S., 1997. Seasonal Variability of Mixed Layer Depth for the World Ocean. NOAA Atlas NESDIS 14, U.S. Gov. Printing Office, Wash., D.C., 96 pp. 87 figs.

PUBLICATIONS (2016-2017)

Hewitt, H.T., M.J. Bell, E.P. Chassignet, A. Czaja, D. Ferreira, S.M. Griffies, P. Hyder, J. McClean, A.L. New, and M.J. Roberts, 2017. Will high-resolution global ocean models benefit coupled predictions on short-range to climate timescales? Ocean Modelling, revised.

Van Sebille, E., S.M. Griffies, R. Abernathey, T.P. Adams, P. Berloff, A. Biastoch, B. Blanke, E.P. Chassignet, Y. Cheng, C.J. Cotter, E. Deleersnijder, K. Döös, H. Drake, S. Drijfhout, S.F. Gary, A.W. Heemink, J. Kjellsson, I.M. Koszalka, M. Lange, C. Lique, G.A. MacGilchrist, R. Marsh, G.C Mayorga Adame, R. McAdam, F. Nencioli, C.B. Paris, M.D. Piggott, J.A. Polton, S. Rühs, S.H. Shah, M.D. Thomas, J. Wang, P.J. Wolfram, L. Zanna, and J.D. Zika, 2017. Lagrangian ocean analysis: Fundamentals and practices. Ocean Modelling, revised.

Clark, M.T., N. Heath, M.A. Bourassa, and E.P. Chassignet, 2017. Quantification of Stokes drift as a mechanism for surface oil advection in the Gulf of Mexico. J. Geophys. Res., revised.

MacKinnon, J.A., M.H. Alford, J.K. Ansong, B.K. Arbic, A. Barna, B.P. Briegleb, F.O. Bryan, M.C. Buijsman, E.P. Chassignet, S. Diggs, P. Gent, S.M. Griffies, R.W. Hallberg, S.R. Jayne, M. Jochum, J.M. Klymak, E. Kunze, W.G. Large, S. Legg, B. Mater, A.V. Melet, L.M. Merchant, R. Musgrave, J.D. Nash, N.J. Norton, A. Pickering, R. Pinkel, K. Polzin, H.L. Simmons, L.C. St. Laurent, O.M. Sun, D.S. Trossman, A.F. Waterhouse, C.B. Whalen, and Z. Zhao, 2017. Climate process team on internal-wave driven ocean mixing. Bull. Amer. Meteor. Soc., doi:10.1175/BAMS-D-16-0030.1, in press.

Treguier, A.M., E.P. Chassignet, A. Le Boyer, and N. Pinardi, 2017. Modeling and forecasting the "weather of the ocean" at the mesoscale. In "THE SEA: THE SCIENCE OF OCEAN PREDICTION", J. Mar. Res., 75, 301-329, doi:10.1357/002224017821836842.

Chassignet, E.P. and X. Xu, 2017. Impact of horizontal resolution (1/12° to 1/50°) on Gulf Stream separation, penetration, and variability. J. Phys. Oceanogr., 47, 1999-2021, doi:10.1175/JPO-D-17-0031.1.

Trossman, D.S., B.K. Arbic, D.N. Straub, J.G. Richman, E.P. Chassignet, A.J. Wallcraft, and X. Xu, 2017. The role of rough topography in mediating impacts of bottom drag in eddying ocean circulation models. J. Phys. Oceanogr., 47, 1941-1959, doi:10.1175/JPO-D-16-0229.1.

Deremble, B., W.K. Dewar, and E.P. Chassignet, 2016. Vorticity dynamics near sharp topographic features. J. Mar. Res., 74, 249-276, doi:10.1357/002224016821744142.

Hiester, H.R., S.L. Morey, D.S. Dukhovskoy, E.P. Chassignet, V.H. Kourafalou, and C. Hu, 2016. A topological approach for quantitative comparisons of ocean model fields to satellite ocean color data. Method. Oceanogr., 17, 232-250, doi:10.1016/j.mio.2016.09.005.

Rosburg, K.C., K.A. Donohue, and E.P. Chassignet, 2016. Three-dimensional model-observation intercomparison in the Loop Current region. Dyn. Atmos. Oceans, 76, 283-305, doi:10.1016/j.dynatmoce.2016.05.001.

Xu, X., P.B. Rhines, and E.P. Chassignet, 2016. Temperature-salinity structure of the North Atlantic circulation and associated heat and freshwater transports. J. Climate, 29, 7723-7741, doi:10.1175/JCLI-D-15-0798.1.

Griffies, S., G. Danabasoglu, P. Durack, A. Alistair, C. Böning, E.P. Chassignet, E. Curchitser, J. Deshayes, H. Drange, B. Fox-Kemper, P. Gleckler, J. Gregory, H. Haak, R. Hallberg, H. Hewitt, D. Holland, T. Ilyina, Y. Komuro, J. Krasting, W. Large, S. Marsland, S. Masina, T. McDougall, J. Orr, A. Pirani, F. Qiao, R. Stouffer, K. Taylor, H. Tsujino, P. Uotila, M. Valdivieso, M. Winton, S. Yeager, V. Balaji, J. Jungclaus, A.M. Treguier, and A.J.G. Nurser, 2016. OMIP contribution to CMIP6: Experimental and diagnostic protocol for the physical component of the Ocean Model Intercomparison Project. Geosci. Model Dev., 9, 3231-3296, doi:10.5194/gmd-2016-77.

Özgökmen,, T.M., E.P. Chassignet, C. Dawson, D. Dukhovskoy, G. Jacobs, J. Ledwell, O. Garcia-Pinada, I. MacDonald, S.L. Morey, M. Olascoaga, A.C. Poje, M. Reed, and J. Skancke, 2016. Over what area did the oil and gas spread during the 2010 Deepwater Horizon oil spill? Oceanography, 29(3), 96-107, http://dx.doi.org/10.5670/oceanog.2016.74.

Tseng, Y., H. Lin, H. Chen, K. Thompson, M. Bentsen, C. Böning, A. Bozec, C. Cassou, E.P. Chassignet, C.H. Chow, G. Danabasoglu, S. Danilov, R. Farneti, P.G. Fogli, Y. Fujii, S.M. Griffies, M. Illicak, T. Jung, S. Masina, A. Navarra, L. Patara, B.L. Samuels, M. Scheinert, D. Sidorenko, C.-H. Sui, H. Tsujino, S. Valcke, A. Voldoire, and Q. Wang, 2016. North and Equatorial Pacific Ocean circulation in the CORE-II hindcast simulations. Ocean Modelling, 104, 143-170, doi:10.1016/j.ocemod.2016.06.003.

Gonçalves, R.C., M. Iskandarani, A. Srinivasan, W.C. Thacker, E.P. Chassignet, and O.M. Knio, 2016. Quantifying uncertainty in an oil-fate model using a polynomial chaos surrogate. J. Geophys. Res., 121, 2058-2077, doi:10.1002/2015JC011311.

National Academies of Sciences, Engineering, and Medicine. 2016. Next Generation Earth System Prediction: Strategies for Subseasonal to Seasonal Forecasts. Washington, DC: The National Academies Press, 290 pp, doi: 10.17226/21873.

Wang Q., M. Ilicak, R. Gerdes, H. Drange, Y. Aksenov, D. Bailey, M. Bentsen, A. Biastoch, A. Bozec, C. Böning, C. Cassou, E.P. Chassignet, A.C. Coward, B. Curry, G. Danabasoglu, S. Danilov, E. Fernandez, P.G. Fogli, Y. Fujii, S.M. Griffies, D. Iovino, A. Jahn, T. Jung, W.G. Large, C. Lee, C. Lique, J. Lu, S. Masina, A.J.G. Nurser, C. Roth, D. Salas y Melia, B.L. Samuels, P. Spence, H. Tsujino, S. Valcke, A. Voldoire, X. Wang, and S.G. Yeager, 2016. An assessment of the Arctic

Ocean in a suite of interannual CORE-II simulations. Part I: Sea ice and solid freshwater. Ocean Modelling, 99, 110-132, doi:10.1016/j.ocemod.2015.12.008.

Wang Q., M. Ilicak, R. Gerdes, H. Drange, Y. Aksenov, D. Bailey, M. Bentsen, A. Biastoch, A. Bozec, C. Böning, C. Cassou, E.P. Chassignet, A.C. Coward, B. Curry, G. Danabasoglu, S. Danilov, E. Fernandez, P.G. Fogli, Y. Fujii, S.M. Griffies, D. Iovino, A. Jahn, T. Jung, W.G. Large, C. Lee, C. Lique, J. Lu, S. Masina, A.J.G. Nurser, C. Roth, D. Salas y Melia, B.L. Samuels, P. Spence, H. Tsujino, S. Valcke, A. Voldoire, X. Wang, and S.G. Yeager, 2016. An assessment of the Arctic Ocean in a suite of interannual CORE-II simulations. Part II: Liquid freshwater. Ocean Modelling, 99, 86-109, doi:10.1016/j.ocemod.2015.12.009.

Ilicak, M., H. Drange, Q. Wang, R. Gerdes, Y. Aksenov, D. Bailey, M. Bentsen, A. Biastoch, A. Bozec, C. Böning, C. Cassou, E.P. Chassignet, A.C. Coward, B. Curry, G. Danabasoglu, S. Danilov, E. Fernandez, P.G. Fogli, Y. Fujii, S.M. Griffies, D. Iovino, A. Jahn, T. Jung, W.G. Large, C. Lee, C. Lique, J. Lu, S. Masina, A.J.G. Nurser, C. Roth, D. Salas y Melia, B.L. Samuels, P. Spence, H. Tsujino, S. Valcke, A. Voldoire, X. Wang, and S.G. Yeager, 2016. An assessment of the Arctic Ocean in a suite of interannual CORE-II simulations. Part III: Hydrography and fluxes. Ocean Modelling, 100, 121-141, doi:10.1016/j.ocemod.2016.02.004.

Dukhovskoy, D.S., P.G. Myers, G. Platov, M.-L. Timmermans, A. Proshutinsky, B. Curry, J.L. Bamber, E.P. Chassignet, X. Hu, C.M. Lee, and R. Somavilla, 2016. Greenland freshwater pathways in the sub-Arctic Seas from model experiments with passive tracers. J. Geophys. Res., 121, 877-907, doi:10.1002/2015JC011290.

Danabasoglu, G., S.G. Yeager, W.M. Kim, E. Behrens, M. Bentsen, D. Bi, A. Biastoch, R. Bleck, C. Böning, A. Bozec, V.M. Canuto, C. Cassou, E.P. Chassignet, A.C. Coward, S. Danilov, N. Diansky, H. Drange, R. Farneti, E. Fernandez, P.G. Fogli, G. Forget, Y. Fujii, S.M. Griffies, A. Gusev, P. Heimbach, A. Howard, T. Jung, M. Kelley, W.G. Large, A. Leboissetier, J. Lu, G. Madec, S.J. Marsland, S. Masina, A. Navarra, A.J.G. Nurser, A. Pirani, A. Romanou, D. Salas y Melia, B.L. Samuels, M. Scheinert, D. Sidorenko, S. Sun, A.-M. Treguier, H. Tsujino, P. Uotila, S. Valcke, A. Voldoire, and Q. Wang, 2016. North Atlantic simulations in Coordinated Ocean-ice Reference Experiments phase II (CORE-II). Part II: Inter-Annual to Decadal Variability. Ocean Modelling, 97, 65-90, doi:10.1016/j.ocemod.2015.11.007.